Original Research Paper | Physics | Volume : 10 | Issue : 05 | May 2025 | e-ISSN : 2456-5040

STRUCTURAL CHANGES IN SHEARS BANDS DUE TO NEUTRON/ PROTON ALIGNMENT

***Amita[1], Veena K. Singh[2]**

[1]Department of Physics, RBS College, Agra, India. (*Corresponding author)
[2]Department of Physics, RBS College, Agra, India.

ABSTRACT

This work has been carried out to understand some salient features of Magnetic Dipole Rotational Bands (MR Bands). We have explained how only a perpendicular coupling of particle-hole configuration at the bandhead can give rise to shears bands by investigating the role of effective interactions between the protons and the neutrons in the shears blades and also from a geometrical picture of various proton-neutron configurations. We have studied the structural changes in these MR bands due to neutron/proton alignments that gave rise to bancrossing and backbending in these bands. From a systematic study of the backbending phenomenon in mass-190 region and the variation of bandcrossing frequency, we have calculated the bandcrossing frequency and spin. For the higher bands, the bandhead spin and energy have been calculated from a second order polynomial fit.

KEYWORDS: Magnetic Rotational Bands, Neutron/Proton Alignment, Configuration Assignment, Backbending, Bandcrossing Frequency

INTRODUCTION

Nuclear high spin states have remained at the center of attraction for both experimental and theoretical studies for the last fifty years. Many new experimental developments in populating and detecting high spin states in nuclei have led to the discovery of several new phenomena in nuclear structure physics. The observation of regular rotational bands, having an I(I+1) dependence of level energies, was among the most interesting and earliest findings. These bands were observed in nuclei that have non spherical distribution of nuclear density. These nuclei are characterized by their large quadrupole moments (axes ratio ~ 1.4 : 1 for normal deformed and 2:1 for super deformed nuclei). Until early 1990's, it was a general belief that only deformed nuclei can exhibit rotational bands. It was therefore a big puzzle for the nuclear physicists when H. Hubel and R. M. Clark [1,2] working independently, observed regular patterns of gamma rays in the near spherical Pb nuclei. A detailed study revealed that the intraband transitions were magnetic dipole (M1) in nature (with very weak or absent crossover electric quadrupole (E2) transitions) in contrast to ND and SD nuclei where the intraband transitions were electric quadrupole (E2) in nature. These bands were therefore named as Magnetic Dipole Rotational (MR) bands. Since then, a large number of these bands have been found in many near spherical nuclei [3,4 and references therein].

The bandhead of all these bands lie at a high excitation energy (a few MeV) and has a high spin (I~ 6-15 ħ), both these features are indicative of a multi quasiparticle configuration of the bandhead. The largest number of these bands have been identified in Pb nuclei, and these, therefore constitute the foremost testing ground for the various physical mechanisms which could give rise to rotational like features with strong magnetic dipole transitions. Since the anisotropic charge density distribution in nuclei results in breaking up of the spherical symmetry which leads to the observation of rotational bands. It is clear that some kind of anisotropy is also playing an important role in the formation of magnetic rotational bands. The "Shears mechanism" proposed by S. Frauendorf [5] provides explanation for the breaking up of spherical symmetry even in nearly spherical nuclei. The anisotropy now exists in current and hence, the magnetic dipole, which rotates about a tilted axis. The bands are therefore, also termed as "shears bands".

The Configuration Assignment:

A configuration assignment of shears bands has been possible in most of the cases based on considerations such as :

1. The excitation energies and angular momenta
2. Comparison with the known excitations in neighboring nuclei and
3. Estimates from model calculations.

The neutron deficient (N < 126) Pb isotopes have 82 protons (filling up the Z=82 shell completely). The low lying excitations of neutron deficient Pb isotopes are known to consist of spherical shell model states arising from neutron hole excitations, and further higher lying excitations are formed on weakly oblate states built on broken- pair proton (particle-hole) excitations across the core. As an example, the 0^+ state at the 931 keV in ^{194}Pb, having a small oblate deformation [6], is built on the $\{\pi 9/2\text{-}\ [505]\}^2$ configuration of the h9/2 orbital. Two high spin isomeric excitations are observed at 2438 keV and 2934 keV having Iπ = 8^+ and 11- respectively [7]; these are interpreted as (2p2h) broken proton pair shell model configurations given by: $[\{\pi h_{9/2}, 9/2\text{-}\ (505)\} \otimes [\{\pi h_{9/2}, 7/2\text{-}\ (514)\}]$ (8+ state) and $[\{\pi h_{9/2}, 9/2\text{-}\ (505)\} \otimes [\{\pi i1_{3/2}, 13/2^+\ (606)\}]$ (11- state). Such a 11- state has also been observed in ^{196}Pb [8], and the g-factor measurement also supports this interpretation. The calculations indicate that the deformation corresponding to this configuration is oblate with $\beta_2 \sim 0.15$ [9]. The 8^+ configuration is also found to be associated with a small oblate deformation from the TRS calculations [10]. However, no regular collective bands built on these 0+, 11- and 8+ states have been observed in any of the even-even Pb isotopes in the range $^{192-202}$Pb where MR bands have been observed. At higher spins, the high-j neutron pairs are also expected to break. The active high-j neutron orbitals in case of neutron deficient Pb isotopes are low - Ω $i_{13/2}$ orbitals.

In mass-130 region, in general, $h_{11/2}$ proton particles combine with $h_{11/2}$ neutron holes to form the bandhead of MR bands. Whereas the MR bands in nuclei in mass-190 region are built upon slightly oblate deformation, the MR bands in mass-130 region exhibit shape coexistence. Most of the bands in this mass region are found to be built on slightly prolate shape but there are bands built on slightly oblate shape as well [3,4]. In mass-110 region, the number of protons and neutrons, both are close to the magic number 50 and hence it is not surprising that many MR bands have been observed in this mass region in many isotopes of Cd, In, Sn and Sb nuclei. The $g_{9/2}$ proton holes and $h_{11/2}$ neutron particles are the active orbitals and are mainly responsible for the formation of MR bands in mass-110 region. The high - Ω $g_{9/2}$ proton holes drive the nucleus towards slightly prolate shape and therefore the MR bands are found to be built on prolate configurations. For the nuclei in mass – 80 region, the active orbitals for both protons and neutrons are the positive parity $g_{9/2}$ orbitals. The nuclei in this mass region have slightly higher deformation and therefore these do not classify as pure magnetic rotors. Instead, we can say that they lie at the beginning of the transitional region between magnetic and conventional collective regions [12].

Shears Mechanism:

The ΔI = 1 bands observed in the lead isotopes have been assigned weakly oblate configurations consisting of the $K^\pi = 11^-$ excitation coupled to low - Ω one/three quasineutrons (in odd-A nuclides) or, two/four quasineutrons (in even-A nuclides) [11]. Since the protons occupy high-Ω states, their density distribution is like a torus with angular momentum pointing along the symmetry axis. The low - Ω neutron hole states, on the other hand, have a dumbbell like density distribution, with angular momentum pointing along a direction perpendicular to symmetry axis [5] (fig. 1 of the report). At the bandhead, the proton angular momentum vector I_π (arising from particles in $h_{9/2}$ and $i_{13/2}$ orbitals) is nearly parallel to the symmetry axis- 3 due to torus like density distribution while the neutron angular momentum I_ν (arising from holes in $i_{13/2}$ subshell) is nearly perpendicular to it due to dumbbell like density distribution.

The total angular momentum vector I then lies along a tilted axis at an angle θ with respect to the symmetry axis. Higher angular momentum states are then generated by aligning I_π and I_ν in a way that resembles the closing of the blades of a pair of shears. This coupling of the proton particles and neutron holes result in a large magnetic dipole μ, which precesses around I. The perpendicular component of μ ($\mu_\perp$), relative to I, decreases in a characteristic manner with the alignment of I_π and I_ν [Fig.1]. The B(M1) values, which are proportional to $\mu_\perp^2$ should also decrease with the closing of the blades of the shears. This behaviour of the B(M1) values is the crucial experimental signature of the shears mechanism. The maximum spin for a configuration is reached when the blades close fully.

From these observations, we can state that the conditions required for shears mechanism to occur in a mass region that is experimentally observable are:

1. A particle hole coupling is generally required
2. The active orbitals must have large j values that can give rise to long regular sequences of states and observable M1 transitions between them.
3. The deformation of the core of the nucleus must be small enough so that the core rotation does not dominate over the shears mechanism.

The above conditions indicate that the regions around doubly magic nuclei are probably the most favorable for the occurrence of shears bands.

Various Possibilities of Neutron-Proton Configurations at The Band Head:

The valence neutrons and protons can have various possible configurations at the bandhead depending on whether they are particles or holes. The particles have a torus-like density distribution and have a maximum overlap with the core if their angular momentum aligns perpendicular to the rotation axis. The holes. on the other hand, have a dumb-bell-like density distribution which aligns the angular momentum of the holes parallel to the rotation axis. Using this concept, the various configurations possible for the neutron-proton alignment depending on whether they are holes or particles have been shown in Fig. 2 (fig. 4 of the report).

1. In figure 2, (a) and (b) denote a near perpendicular coupling of proton particle-neutron hole (a) and neutron particle-proton hole (b). The components of the proton and neutron magnetic moments perpendicular to total angular momentum add up to give a resultant magnetic moment which precesses around the total angular momentum breaking the rotational symmetry and gives rise to shears bands.

2. Figures (c) and (d) show a pair of proton particles/holes (c) and a pair of neutron particles/holes (d) in time reversed states which give rise to a total angular momentum along the symmetry axis of the core. It is seen that the perpendicular components of proton and neutron magnetic moments cancel and as a result such a configuration cannot give rise to shears bands.

3. Figures (e) and (f) show the near perpendicular coupling of a proton particle with a proton hole (e) and a neutron particle with a neutron hole (f). In this case the components of the magnetic moments of proton and neutron which are perpendicular to the total angular momentum cancel if the angular momentum of the particle and hole are equal and no MR bands are observed. Even if the particle and hole blades have different

angular momentum, the resultant is very small that the shears mechanism is easily dominated by the core rotation and shears bands are very difficult to observe.

4. Figures (g) and (h) show the proton and neutron particle hole in time reversed states. In this case, if the proton and neutron angular momentum are the same, then the total angular momentum will lie in a direction parallel to the symmetry axis. The perpendicular components of proton and neutron angular momentum add up to give a resultant which is also perpendicular to symmetry axis. Due to this, the rotation of about I do not break the rotational symmetry and so does not give rise to magnetic rotation.

Proton/Neutron Alignment:
Each shears band is built on a particular configuration of valence protons and neutrons. It may sometimes happen that an additional pair of protons or neutrons break up and occupy a higher state. This new configuration can give rise to a new shears band. The observation of backbending is very common in the high spin states of normal deformed bands. Since the shears bands are also high spin bands, the observation of backbending is not a surprising feature in these bands. The phenomenon of backbending is normally attributed to the crossing of two rotational bands in normal deformed nuclei [13]. It means that at certain $I=I_{cross}$, the energies of the two states belonging to different bands are approximately equal. The band after the crossing has an extra pair of aligned protons/neutrons. Such a crossing leads to a rearrangement in the intrinsic structure of the deexciting nucleus.

In figure 3, we plot spin I vs. gamma ray energies (E_γ) for the bands in Pb isotopes in A=195 mass region for the bands that exhibit backbending. We find that, in case of all the bands, initially we observe a smooth rising plot. It means gamma ray energies rise smoothly with increasing spin. However, at a certain spin, we observe a sharp change in the shape of the plots and then we again observe a smooth rise in gamma ray energies. The data listed here has been taken from [4] and the references therein.

The configurations for all these bands, as given in the literature, are listed in Table 1. Here we observe that whereas most of the time it is the alignment of a pair of $i_{13/2}$ neutron holes that leads to backbending. In some cases, it is the $f_{5/2}p_{3/2}$ neutron pair responsible for the occurrence of backbending. Since the number of proton/neutron particles or holes changes after the crossing, the relative lengths of the shears blades also differ before and after the crossing. So the blades reorient by increasing the shears angle to produce a state with the same angular momentum at lower energy. It is interesting to note that the second band which crosses the first band is also a shears band because the two blades of shears, which were beginning to close with the rising spin in the lower shears band, again open up in the higher lying shears band and the shears mechanism becomes active once again.

In figure 4, we plot the excitation energies vs. spin for all the bands under consideration, to calculate the band crossing frequency and spin. The higher lying shears band has a configuration with an additional pair of neutron hole alignment. We have done a second order polynomial fit on these bands and from the minimum of the curve, the bandhead spin and energies are calculated. From the crossing point of the two bands, the bandcrossing spin and energy has also been calculated. These are presented in Table 2. These calculations present a simple but lucid interpretation for the systematic study of shears bands in mass-190 region.

CONCLUSION
In the present paper, we have studied some interesting phenomenon associated with the magnetic dipole rotational bands. As these bands are not the normal rotational bands arising from the anisotropic charge distribution, the configuration assignment plays an important role in understanding the formation of these bands observed in low deformed nuclei. We have presented various possibilities of neutron proton configurations at the bandhead and find that a particle- hole coupling is essential to observe the shears bands. Another phenomenon that we have discussed here, is the backbending observed in some of these bands. We have taken mass-190 region for our present studies and find that the phenomenon is observed as a result of the bandcrossing due to the alignment of an extra pair of proton/neutron. We have done a second order polynomial fit, in order to determine the bandcrossing frequencies and energies.

REFERENCES

1. H. Hübel et al., Prog. Part. Nucl. Phys. 28, 427 (1992)
2. R. M. Clark et al., Phys. Lett. B 275, 247 (1992)
3. Amita, A.K. Jain and Balraj Singh, Atomic Data and Nuclear Data Tables 74, 283 (2000)
4. Sushil Kumar et al., https://doi.org/10.48550/arXiv.2303.00499 (2023)
5. S. Frauendorf, Nucl. Phys. A 557, 259c (1993)
6. P. Van Duppen et al., Phys. Rev. Lett. 52, 1974 (1984)
7. M. G. Porquet et al., Journal of Physics G 20, 765 (1994)
8. J. Penninga et al., Nucl. Phys. A 471, 535 (1987)
9. E. F. Moore et al., Phys. Rev. C 51, 115 (1995)
10. R. M. Clark et al., Nucl. Phys. A 562, 121 (1993)
11. S. Chmel, S. Frauendorf and H. Hübel, Phys. Rev. C 75, 044309 (2007)
12. Amita et al., Phys. Rev. C64, 034308 (2001)
13. R. Bengtsson and S. Frauendorf, Nucl. Phys. A314, 27 (1979)
14. R. M. Clark and A. O. Macchiavelli, Ann. Rev. Nucl. Part. Sci. 50, 1 (2000)
15. A. O. Macchiavelli et al., Phys. Rev. C57, R1073 (1998)
16. A. O. Macchiavelli et al., Phys. Rev. C58, 3746 (1998)

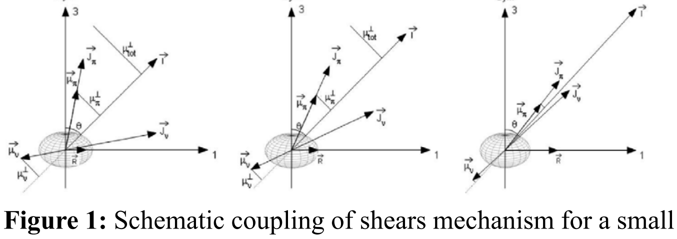

Figure 1: Schematic coupling of shears mechanism for a small oblate deformation in the Pb region at low spin (left), at higher intermediate spin (middle), and at maximum spin (right)

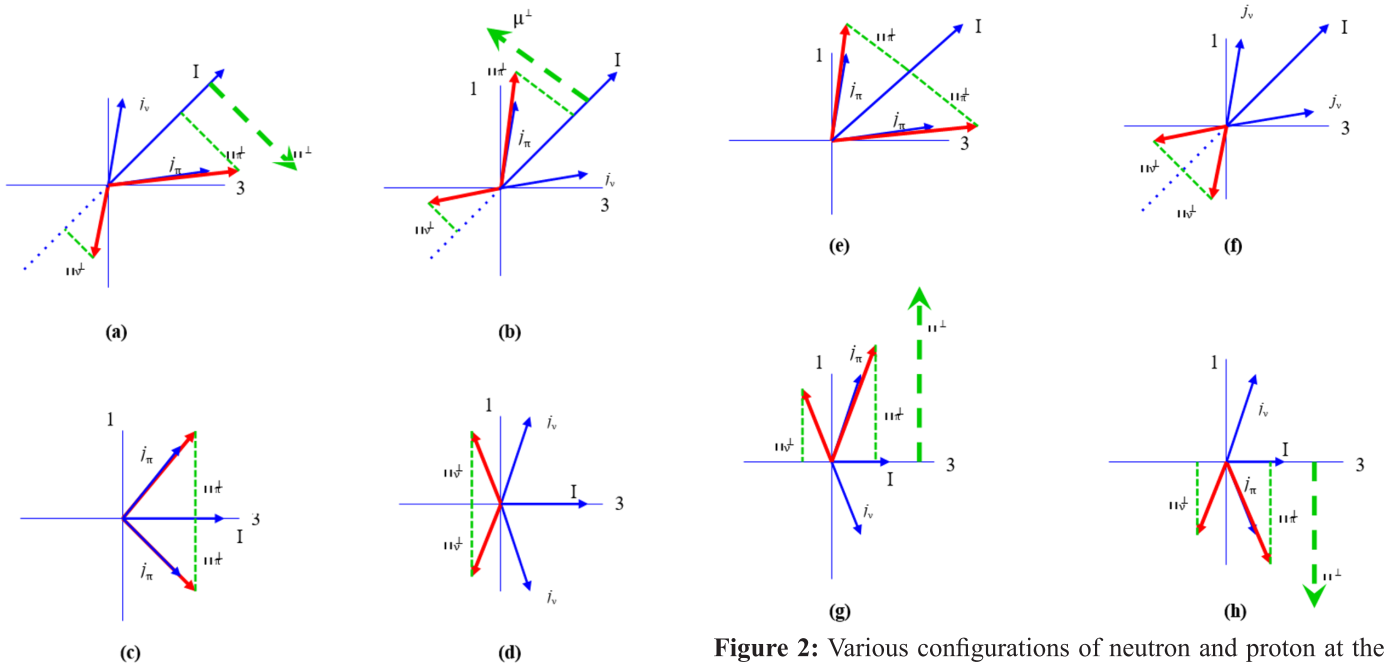

Figure 2: Various configurations of neutron and proton at the bandhead

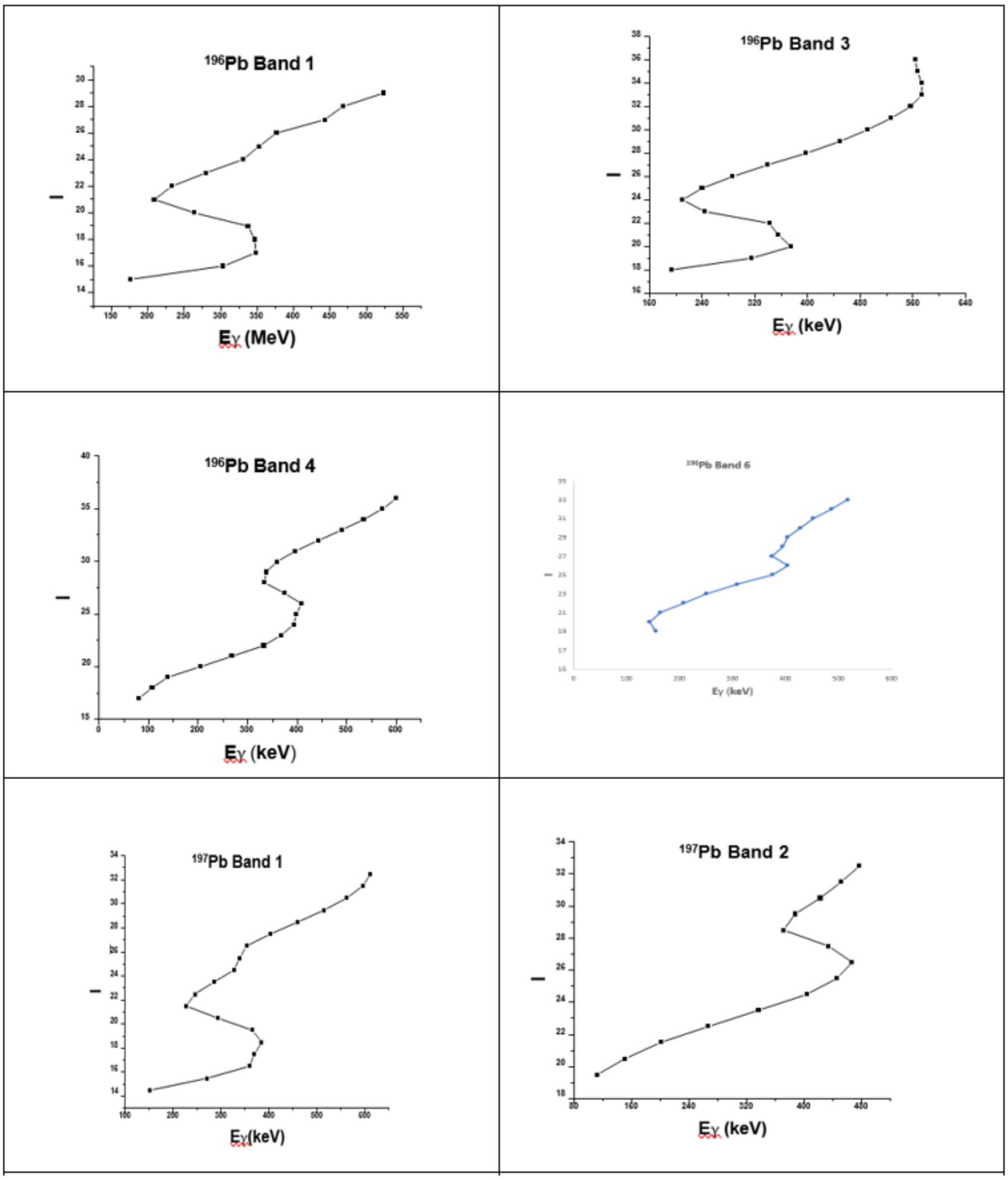

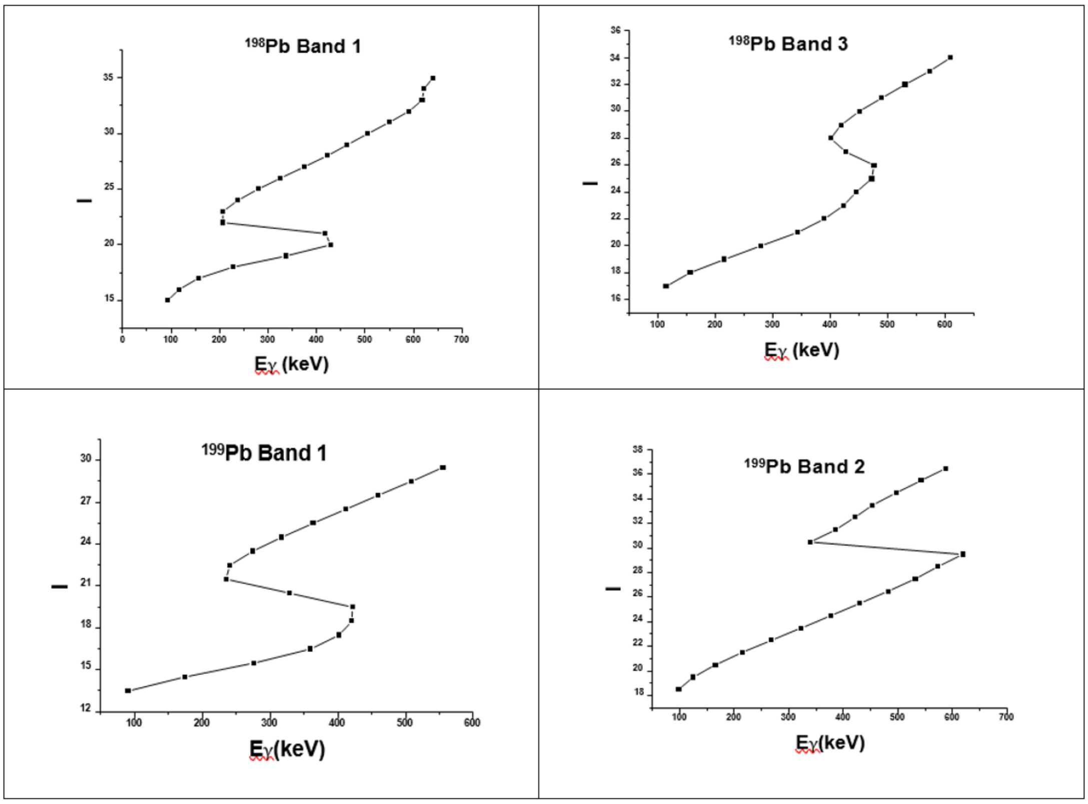

Figure 3: Plot of spin vs. E_γ for various bands in mass 195 region in Pb nuclei showing backbending

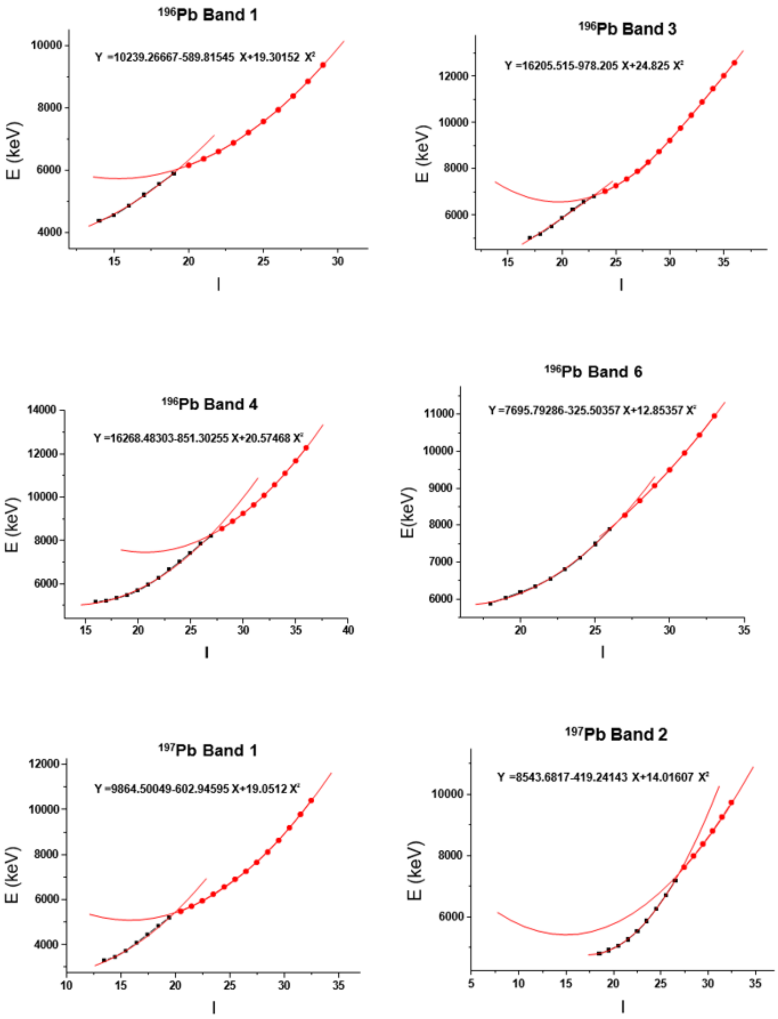

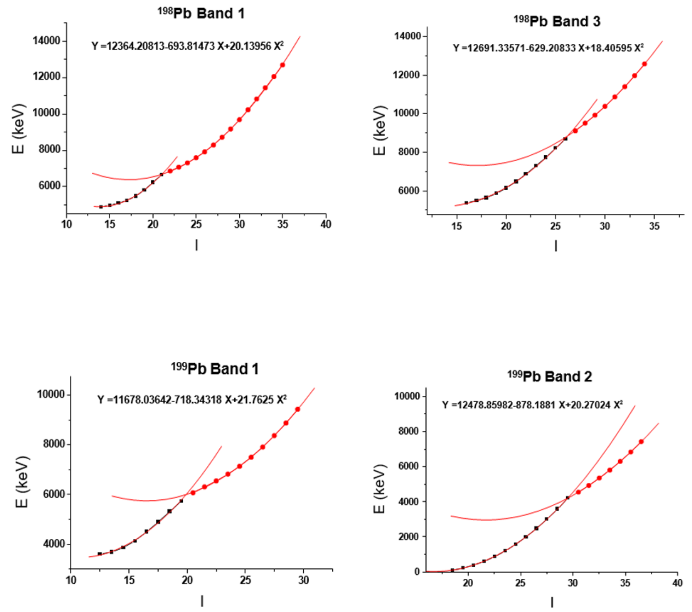

Figure 4: Plot of excitation energy vs. spin I for the shears bands under consideration

Nuclei	Band	Configuration
^{190}Hg	2	$\pi\,(h_{9/2}\,h^{-1}_{11/2})$ with a few holes in $\nu\,(i_{13/2})$ and a few particles in $\nu\,(p_{3/2}, f_{5/2}, p_{1/2})$ and remaining holes in $\nu\,(h_{9/2}, f_{7/2})$ levels
^{193}Hg	2	$\pi\,(h^2_{9/2}h^{-2}_{11/2})\nu\otimes(i^3_{13/2})$
^{195}Hg	2	$\pi\,(h^2_{11/2})\nu\otimes(i^{-3}_{13/2})$
^{191}Pb	1	$\pi\,(h_{9/2}i_{13/2}s^{-2}_{1/2})_{K=11-}\otimes\nu(i^{-1}_{13/2})$below and $\pi\,(h_{9/2}i_{13/2}s^{-2}_{1/2})_{K=11-}\otimes\nu(i^{-3}_{13/2})$ above band crossing
^{192}Pb	1	$\pi\;(9/2[505]\otimes 13/2[606])_{K=11-}\otimes\nu\;(i^2_{13/2})$
	2	$\pi\;(7/2[514]\otimes 13/2[606])_{K=11-}\otimes\nu\;(i^2_{13/2})$
^{193}Pb	1	$\pi\;(9/2[505]\otimes 13/2[606])_{K=11-}\otimes\nu\;(i^2_{13/2}\,p_{5/2})$
	2	$\pi\;(9/2[505]\otimes 13/2[606])_{K=11-}\otimes\nu\;(i^2_{13/2}\,f_{5/2})$
	3	$\pi\;(9/2[505]\otimes 13/2[606])_{K=11-}\otimes\nu\;(i^2_{13/2})$
	4	$\pi\;(9/2[505]\otimes 13/2[606])_{K=11-}\otimes\nu\;(i^3_{13/2})$
^{194}Pb	1	$\pi\,(9/2[505]\otimes 13/2[606])_{K=11-}\otimes\nu\{i_{13/2}(p_{3/2}f_{5/2})^1\}$
	2	$\pi\,(9/2[505]\otimes 7/2[514])_{K=8+}\otimes\nu\,(i^2_{13/2})$ at low spin and $\pi\,(9/2[505]\otimes 7/2[514])_{K=8+}\otimes\nu\,(i^4_{13/2})$ at higher spin
	3	$\pi\,(9/2[505]\otimes 7/2[514])_{K=11-}\otimes\nu\,(i^2_{13/2})$ before and $\pi\,(9/2[505]\otimes 13/2[606])_{K=11-}\otimes\nu\,(i^4_{13/2})$ after the up-bending
	4	$\pi\,(9/2[505]\otimes 13/2[606])_{K=11-}\otimes\nu\,(i^2_{13/2})$
	7	$\pi\,(9/2[505]\otimes 13/2[606])_{K=11-}\otimes\nu\{i_{13/2}(f_{5/2}\,i_{13/2})^1\}$
^{195}Pb	1	$\pi\,(9/2[505]\otimes 13/2[606])_{K=11-}\otimes\nu(i^1_{13/2})$
	2	$\pi\,(9/2[505]\otimes 13/2[606])_{K=11-}\otimes\nu\,(i^3_{13/2})$
	3	$\pi\,(9/2[505]\otimes 13/2[606])_{K=11-}\otimes\nu\,(i^2_{13/2}(f_{5/2}\,p_{3/2})^1)$ at low spin and $\pi\,(9/2[505]\otimes 13/2[606])_{K=11-}\otimes\nu\,(i^4_{13/2}\,(f_{5/2}\,p_{3/2})^1)$ at high spin
^{196}Pb	1	$\pi\,(h^2_{9/2})_{K=8+}\otimes\nu\{i^{-1}_{13/2}\,(f_{5/2}\,p_{3/2})^1\}$ before and $\pi\,(h^2_{9/2})_{K=8+}\otimes\nu\{i^{-3}_{13/2}\,(f_{5/2}\,p_{3/2})^1\}$ after band crossing
	3	$\pi\,(i_{13/2}\,h_{9/2})_{K=11-}\otimes\nu\{i^{-1}_{13/2}\,(f_{5/2}\,p_{3/2})^1\}$ before and $\pi\,(i_{13/2}\,h_{9/2})_{K=11-}\otimes\nu\{i^{-3}_{13/2}\,(f_{5/2}\,p_{3/2})^1\}$ after band crossing
	4	$\pi\,(i_{13/2}\,h_{9/2})_{K=11-}\otimes\nu(i^{-2}_{13/2})$ before and $\pi\,(i_{13/2}\,h_{9/2})_{K=11-}\otimes\nu(i^{-4}_{13/2})$ after band crossing
	6	$\pi\,(i_{13/2}\,h_{9/2})_{K=11-}\otimes\nu\{i^{-2}_{13/2}\,(f_{5/2}\,p_{3/2})^2\}$ before and $\pi\,(i_{13/2}\,h_{9/2})_{K=11-}\otimes\nu\{i^{-2}_{13/2}\,(f_{5/2}\,p_{3/2})^4\}$ after band crossing

	7	$\pi (i_{13/2} h_{9/2})_{K=11-} \otimes \nu\{i^{-3}_{13/2} (f_{5/2} p_{3/2})^{1}\}$ before and $\pi (i_{13/2} h_{9/2})_{K=11-} \otimes \nu\{i^{-2}_{13/2} (f_{5/2} p_{3/2})^{4}\}$ after band crossing
^{197}***Pb***	1	$\pi (i_{13/2} h_{9/2})_{K=11-} \otimes \nu(i^{-1}_{13/2})$ before and $\pi (i_{13/2} h_{9/2})_{K=11-} \otimes \nu(i^{-3}_{13/2})$ after band crossing
	2	$\pi (i_{13/2} h_{9/2})_{K=11-} \otimes \nu(i^{-2}_{13/2} f^{-1}_{5/2})$ before and $\pi (i_{13/2} h_{9/2})_{K=11-} \otimes \nu(i^{-4}_{13/2} f^{-1}_{5/2})$ above band crossing
	4	$\pi (i_{13/2} h_{9/2}) \otimes \nu (i^{-3}_{13/2} f^{-2}_{5/2})$
	5	$\pi (i_{13/2} h_{9/2})_{K=11-} \otimes \nu\{i^{-2}_{13/2} (f_{5\,2} p_{3/2})^{-3}\}$
^{198}***Pb***	1	$\pi (i_{13/2} h_{9/2})_{K=11-} \otimes \nu(i^{-1}_{13/2} f^{-1}_{5/2})$ before and $\pi (i_{13/2} h_{9/2})_{K=11-} \otimes \nu(i^{-3}_{13/2} f^{-1}_{5/2})$ above first band crossing
	2	$\pi (i_{13/2} h_{9/2})_{K=11-} \otimes \nu\{i^{-2}_{13/2} (f_{5/2} p_{3/2})^{-2}\}$ before and $\pi (i_{13/2} h_{9/2})_{K=11-} \otimes \nu(i^{-4}_{13/2} (f_{5/2} p_{3/2})^{-2}\}$ above first band crossing
	3	$\pi (i_{13/2} h_{9/2})_{K=11-} \otimes \nu (i^{-2}_{13/2})$ before and $\pi (i_{13/2} h_{9/2})_{K=11-} \otimes \nu (i^{-4}_{13/2})$ after band crossing
	4	$\pi (i_{13/2} h_{9/2})_{K=11-} \otimes \nu\{i^{-2}_{13/2} (f_{5/2} p_{3/2})^{-2}\}$ before and $\pi (i_{13/2} h_{9/2})_{K=11-} \otimes \nu(i^{-4}_{13/2} (f_{5/2} p_{3/2})^{-2}\}$ after band crossing
	5	$\pi (i_{13/2} h_{9/2})_{K=11-} \otimes \nu (i^{-1}_{13/2} p^{-1}_{3/2})$ before and $\pi (i_{13/2} h_{9/2})_{K=11-} \otimes \nu (i^{-3}_{13/2} p^{-1}_{3/2})$ after band crossing
^{199}***Pb***	1	$\pi (i_{13/2} h_{9/2})_{K=11-} \otimes \nu (i^{-1}_{13/2})$ before and $\pi (i_{13/2} h_{9/2})_{K=11-} \otimes \nu (i^{-3}_{13/2})$ after band crossing
	2	$\pi (i_{13/2} h_{9/2})_{K=11-} \otimes \nu (i^{-2}_{13/2} f^{-1}_{5/2})$ before and $\pi (i_{13/2} h_{9/2})_{K=11-} \otimes \nu (i^{-4}_{13/2} f^{-1}_{5/2})$ after band crossing
	3	$\pi (i_{13/2} h_{9/2})_{K=11-} \otimes \nu (i^{-2}_{13/2} f^{-1}_{5/2})$
^{200}***Pb***	1	$\pi (i_{13/2} h_{9/2})_{K=11-} \otimes \nu (i^{-2}_{13/2})$
^{201}***Pb***	2	$\pi (i_{13/2} h_{9/2})_{K=11-} \otimes \nu (i^{-2}_{13/2} p^{-1}_{3/2})$
^{197}***Bi***	1	$\pi (i_{13/2} h^{2}_{9/2})_{K=14.5} \otimes \nu\{i_{13/2} (p_{3/2} f_{5/2})^{1}\}$
^{198}***Bi***	1	$\pi (i_{13/2} h_{9/2} s^{-1}_{1/2}) \otimes \nu(i^{-4}_{13/2} p^{-1}_{3/2})$
^{199}***Bi***	1	$\pi (i_{13/2} h_{9/2} s^{-1}_{1/2}) \otimes \nu(i^{-2}_{13/2})$
^{200}***Bi***	1	$\pi (i_{13/2} h_{9/2} s^{-1}_{1/2}) \otimes \nu(i^{-1or3}_{13/2})$
	2	$\pi (i_{13/2} h_{9/2} s^{-1}_{1/2}) \otimes \nu(i^{-1or3}_{13/2})$
^{202}***Bi***	1	$\pi (i_{13/2} h_{9/2} s^{-1}_{1/2}) \otimes \nu(i^{-1or3}_{13/2})$
	2	$\pi (i_{13/2} h_{9/2} s^{-1}_{1/2})$ or $\pi(h^{2}_{9/2}\, s^{-1}_{1/2}) \otimes \nu (i^{-1or3}_{13/2})$
^{203}***Bi***	1	$\pi (i_{13/2} h_{9/2} s^{-1}_{1/2}) \otimes \nu (i^{-1or3}_{13/2})$
^{205}***Rn***	1	$\pi (i^{2}_{13/2}) \otimes \nu (i_{13/2})$
^{204}***At***	1	Proposed to be $\pi (h_{9/2}) \otimes \nu (i_{13/2})$
^{206}***Fr***	1	Proposed to be $\pi (h_{9/2}) \otimes \nu (i_{13/2})$

Table 1: Configurations in A=195 mass region

Nuclide	Band	Bandcrossing spin	Bandcrossing energy (keV)	Bandhead spin	Bandhead energy
^{196}*Pb*	**1**	**19.35**	**6057.86**	**15**	**5733.51**
	3	**22.87**	**6822.01**	**20**	**6568.49**
	4	**26.91**	**8264.22**	**21**	**7465.5**
	6	**26.54**	**8111.37**	**17**	**5855.83**
^{197}*Pb*	**1**	**19.95**	**5423.18**	**31/2**	**5094.31**
	2	**26.91**	**7419.98**	**29/2**	**5408.96**
^{198}*Pb*	**1**	**21.05**	**6693.21**	**17**	**6392.84**
	3	**26.2**	**8847.69**	**18**	**7318.85**
^{199}*Pb*	**1**	**19.91**	**6005.82**	**33/2**	**5750.86**
	2	**29.49**	**4212.07**	**43/2**	**2967.66+X**

Table 2: Band crossing spin and energy and bandhead spin and energy of MR bands of Pb